



Supplement of

Trace gas composition in the Asian summer monsoon anticyclone: a case study based on aircraft observations and model simulations

Klaus-D. Gottschaldt et al.

Correspondence to: Klaus-D. Gottschaldt (klaus-dirk.gottschaldt@dlr.de)

The copyright of individual parts of the supplement might differ from the CC-BY 3.0 licence.

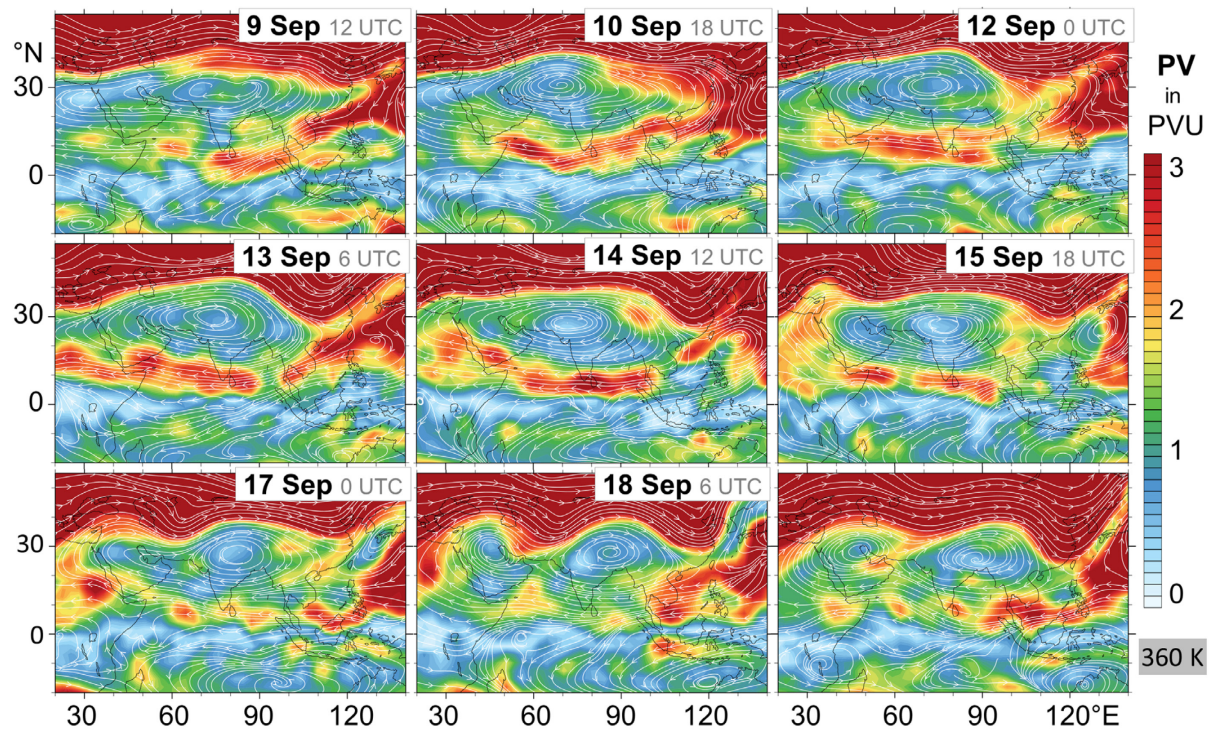


Figure S1: Streamlines and potential vorticity (PV) at the 360 K isentropic level as simulated by EMAC for selected output time steps in September 2012.

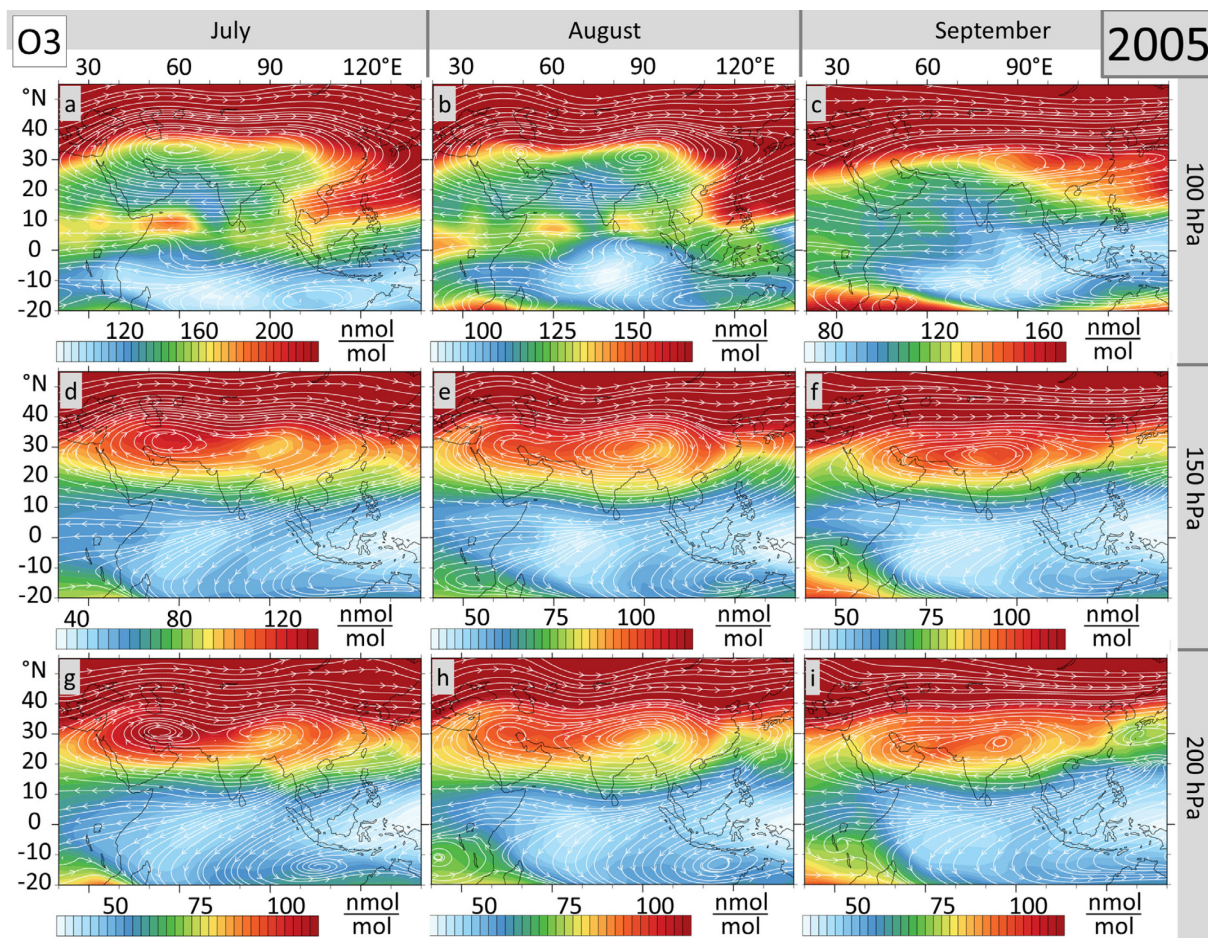


Figure S2: Monthly mean O₃ mixing ratios and streamlines in the ASMA region as simulated by EMAC for different pressure altitudes. The year 2005 was chosen for comparability with Park et al. (2007), who reported an O₃ minimum in the ASMA at 100 hPa for July – August 2005 (based on MLS satellite data). That feature is reproduced by EMAC, but O₃ is increased in the ASMA at lower altitudes.

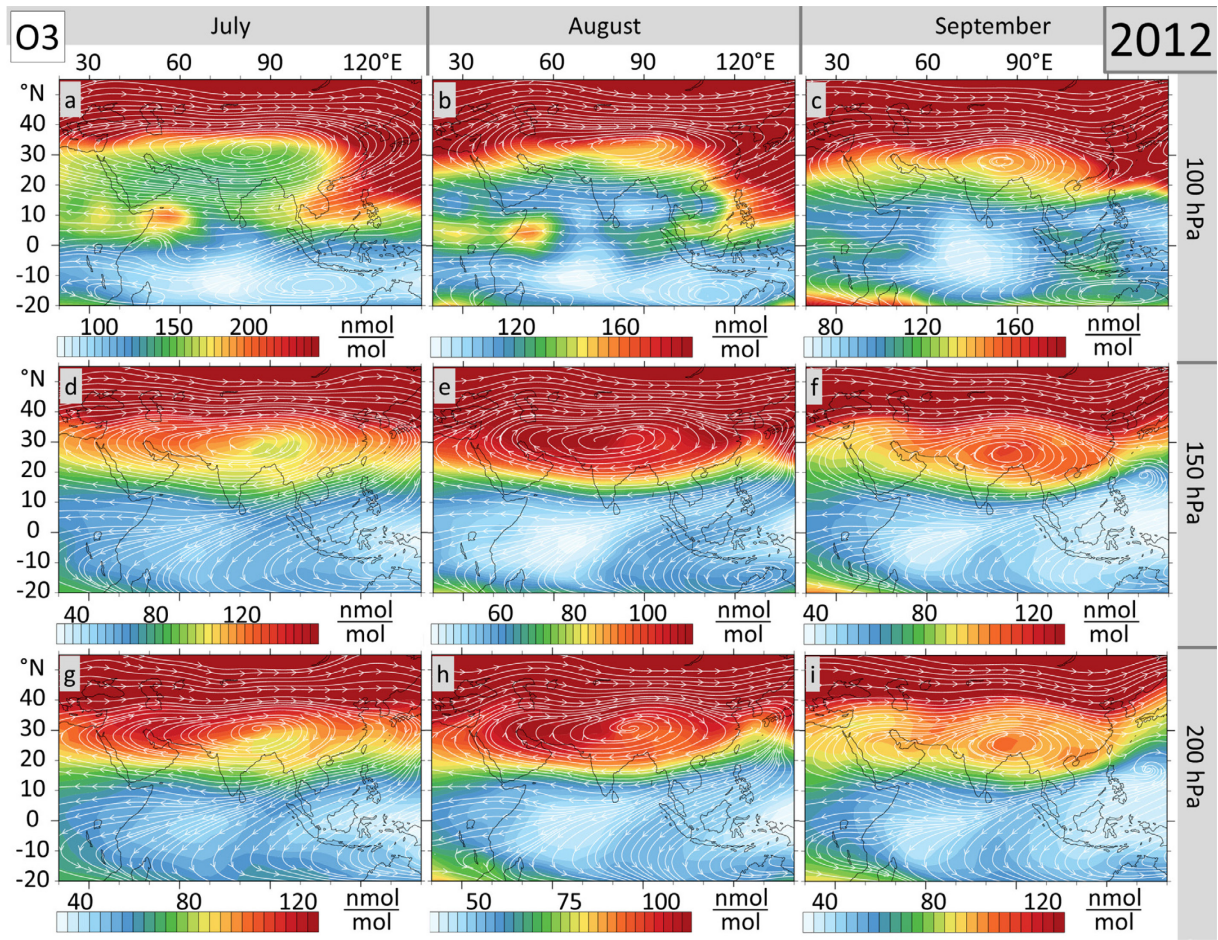


Figure S3: As Fig. S1, but for the year 2012. The main features are almost identical to 2005 (Fig. S1). O_3 is locally decreased in the ASMA only in July and August at 100 hPa. There are enhanced O_3 mixing ratios at lower altitudes throughout the monsoon season.

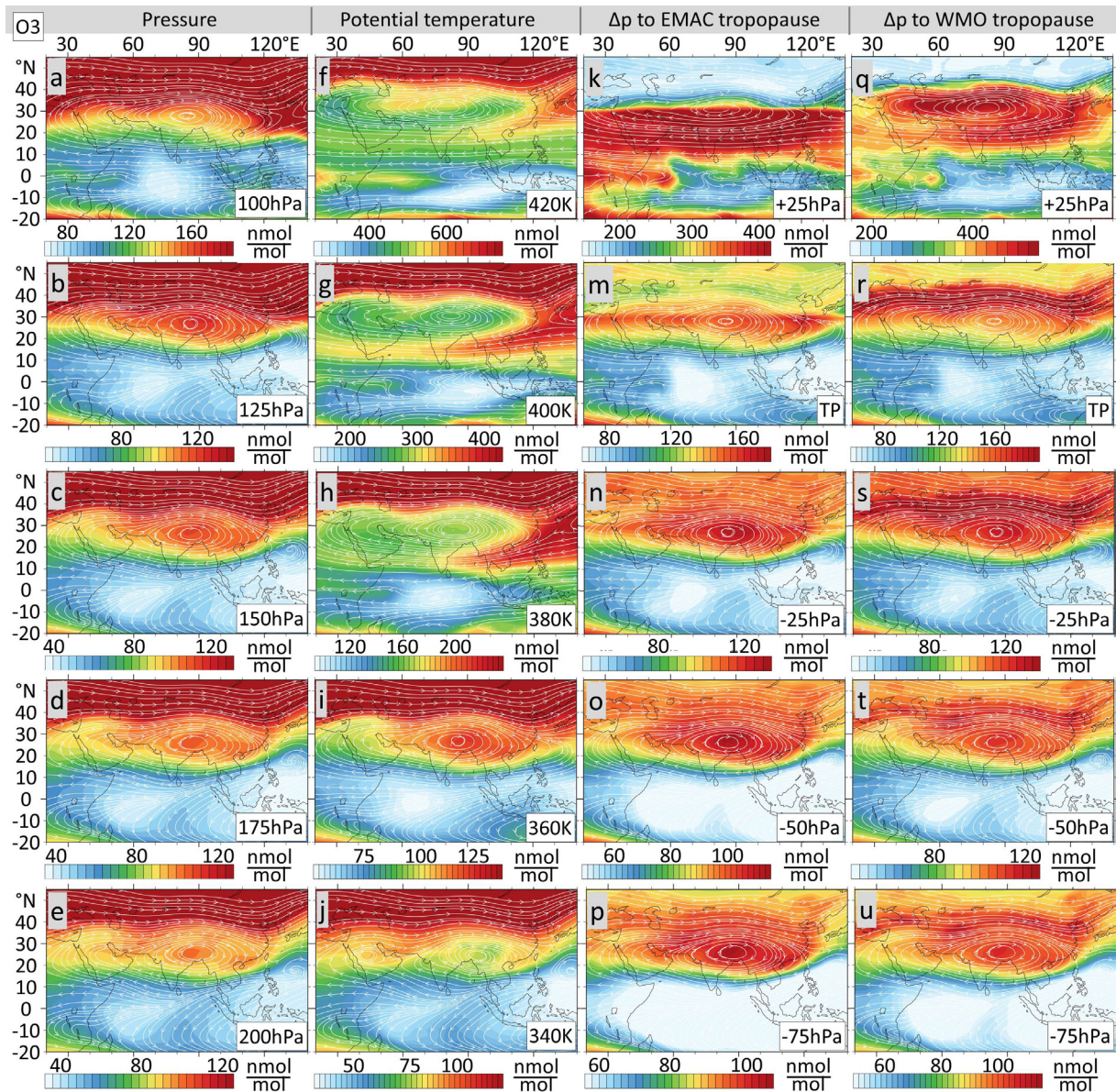


Figure S4: Monthly mean streamlines and O₃ mixing ratios in the ASMA region as simulated by EMAC for September 2012. Various levels are shown in different vertical coordinates to highlight two peculiarities. (i) Some studies report decreased O₃ in the ASMA interior on isentropic surfaces (Randel and Park, 2006; Kunze et al., 2010), while other analyses are on pressure levels (Park et al., 2007). Due to diabatic heating over the Tibetan Plateau, isentropes are concave there. They essentially form a trough when viewed in pressure coordinates (Ren et al., 2014). Thus it is more likely to find lower tropospheric trace gas signatures in the ASMA interior on a potential temperature surface than on a pressure level. (ii) The TP in EMAC is defined according to the WMO definition between 30°S and 30°N, and at a potential vorticity surface of 3.5 PVU otherwise. This might lead to discontinuities when viewing the ASMA region in terms of pressure distance (Δp) to the TP.

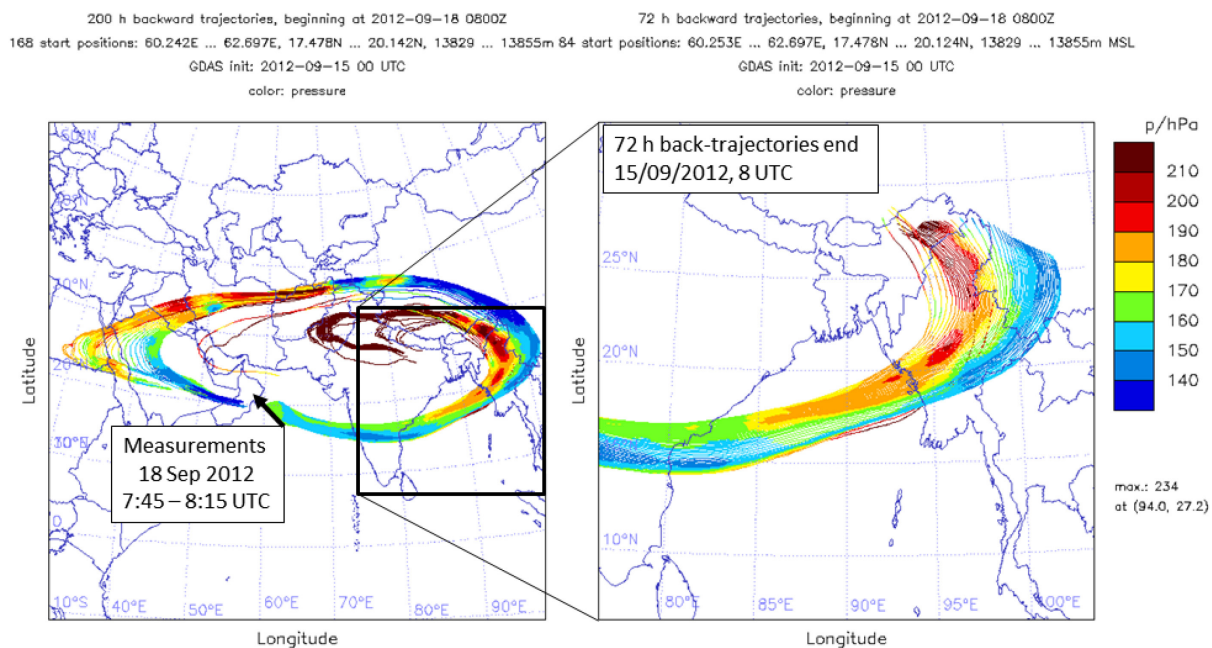


Figure S5: 200 hour (left panel) and 72 hour (right panel) backward trajectories with initial positions corresponding to 10 s steps along the HALO flight track during POI3. Colors indicate the pressure altitude of air parcels. UT anticyclonic circulation was entrained by a lower tropospheric upwelling at the eastern ASMA flank at about 15 September 2012, 8 UTC. Going back 72 hours, the transect measured by HALO corresponds approximately to an inclined zonal transect at 27°N.

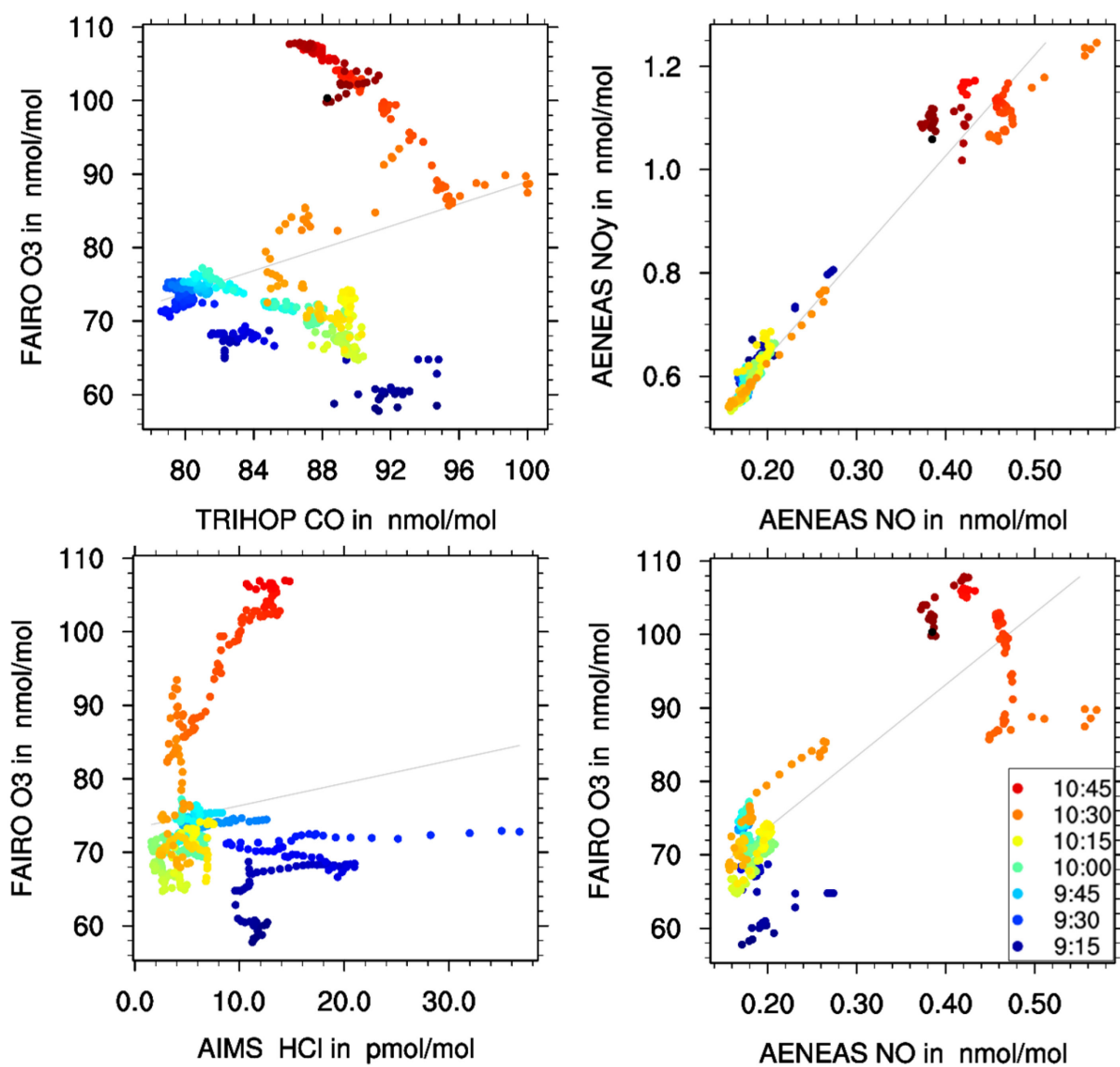


Figure S6: Tracer-tracer relations in the ASMA, as observed during POI5. Colors indicate the time of measurement, grey lines are linear fits to the data. These panels are shown here for completeness, to document the in-situ data for all POIs. They may be explained by the same processes discussed for POI3 in the main text, but are better viewed in the more climatological context of Gottschaldt et al. (2017).

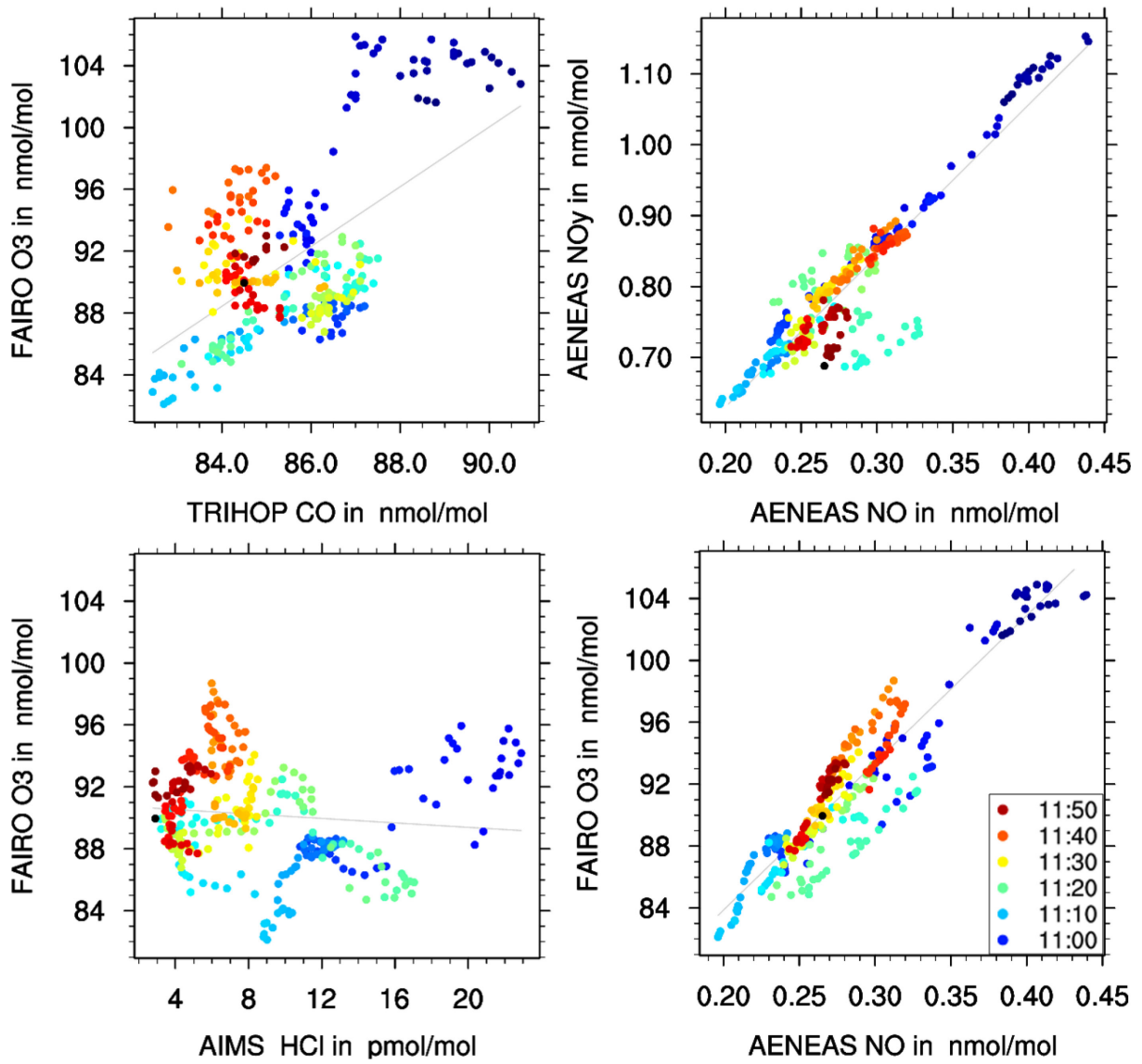


Figure S7: As Fig. S5, but for POI6.

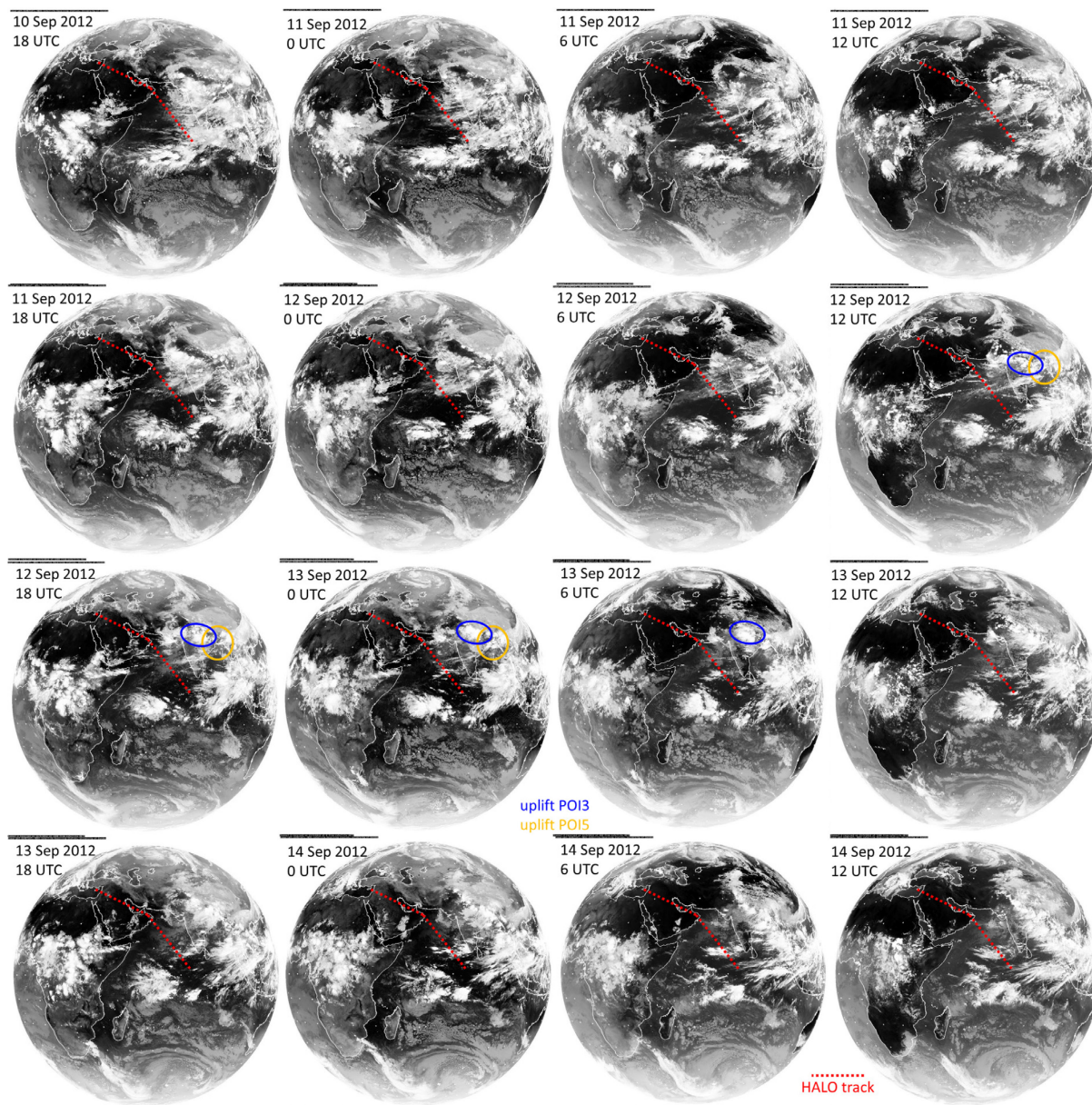


Figure S8: Meteosat-7 (positioned 57°E, Indian Ocean Data Coverage) quicklook images for the period 10 – 18 September 2012 (continued on next page). The thermal infra-red channel (10.5 – 12.5 μm) is shown. Dark shadings correspond to cloud-free conditions, which prevailed at the HALO flight track during the entire period. Light shadings east of India indicate convection, which is consistent with upwellings at the eastern flank of the ASMA that were also seen in the corresponding back-trajectories (Figs. 4, A4). The positions of the air masses encountered during POI3/5 are marked blue/orange in the panels corresponding to the uplift. All images are courtesy of the NERC Satellite Receiving Station, Dundee University, Scotland (www.sat.dundee.ac.uk).

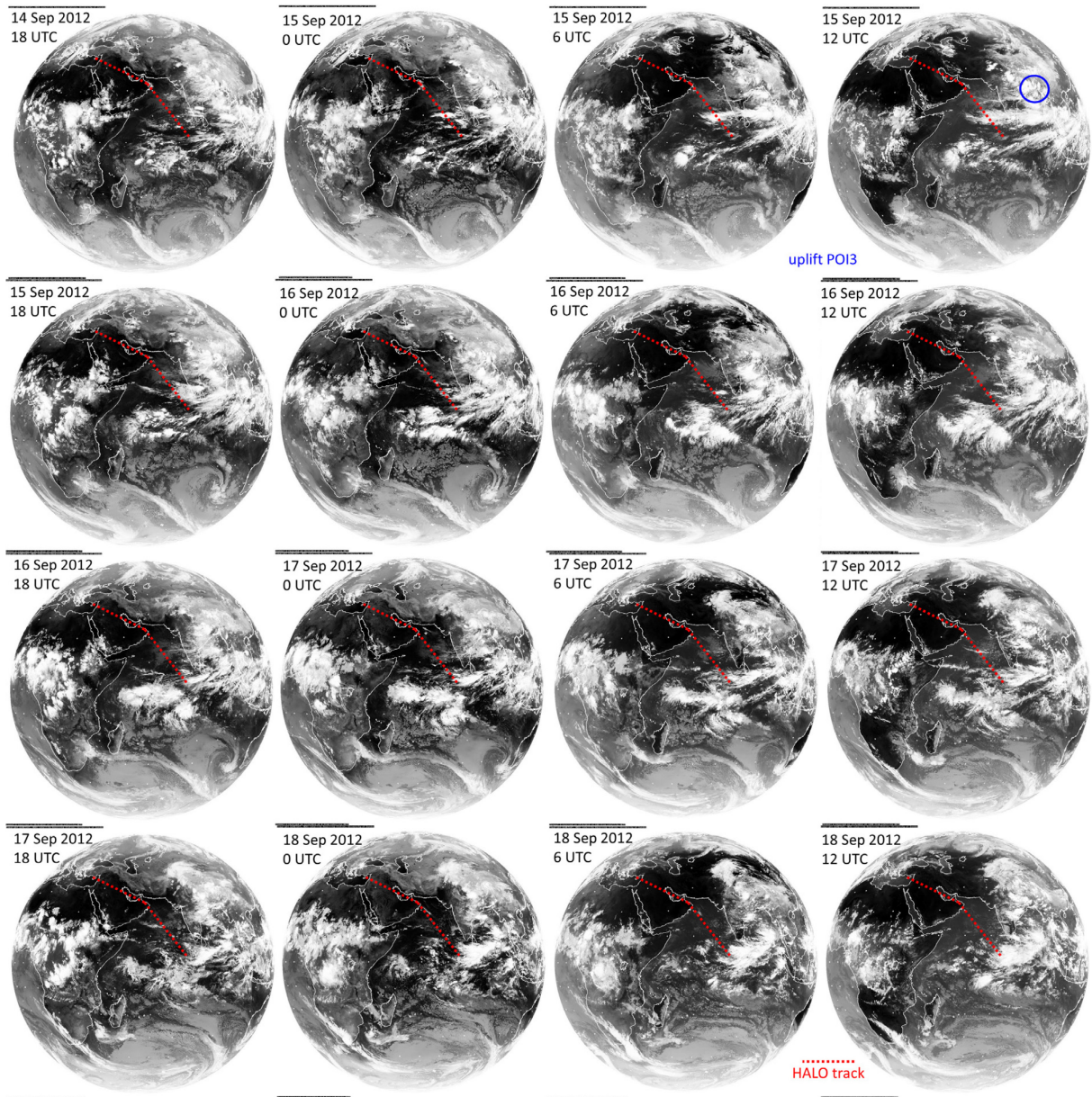


Figure S8 continued

References

- Gottschaldt, K., Schlager, H., Baumann, R., Cai, D. S., Eyring, V., Graf, P., Grewe, V., Jöckel, P., Jurkat, T., Voigt, C., Zahn, A., and Ziereis, H.: Working title: Interplay of dynamics and composition in the Asian summer monsoon anticyclone, *Atmos. Chem. Phys. Discuss.*, in prep., 2017.
- Kunze, M., Braesicke, P., Langematz, U., Stiller, G., Bekki, S., Brühl, C., Chipperfield, M., Dameris, M., Garcia, R., and Giorgetta, M.: Influences of the Indian Summer Monsoon on Water Vapor and Ozone Concentrations in the UTLS as Simulated by Chemistry–Climate Models, *Journal of Climate*, 23, 3525-3544, 10.1175/2010jcli3280.1, 2010.
- Park, M., Randel, W. J., Gettelman, A., Massie, S. T., and Jiang, J. H.: Transport above the Asian summer monsoon anticyclone inferred from Aura Microwave Limb Sounder tracers, *Journal of Geophysical Research*, 112, 10.1029/2006jd008294, 2007.
- Randel, W. J., and Park, M.: Deep convective influence on the Asian summer monsoon anticyclone and associated tracer variability observed with Atmospheric Infrared Sounder (AIRS), *Journal of Geophysical Research*, 111, 10.1029/2005jd006490, 2006.
- Ren, R., Wu, G., Cai, M., Sun, S., Liu, X., and Li, W.: Progress in Research of Stratosphere-Troposphere Interactions: Application of Isentropic Potential Vorticity Dynamics and the Effects of the Tibetan Plateau, *J. Meteor. Res.*, 28, 714-731, 10.1007/s13351-014-4026-2, 2014.